Eur. Phys. J. B **16**, 245–250 (2000)

THE EUROPEAN PHYSICAL JOURNAL B

EDP Sciences

Submillimeter and infrared spectroscopy on $La_{0.85}Sr_{0.15}MnO_3$

A. Paolone[1,a], P. Roy[1,b], A. Pimenov[2,c], A. Loidl[2], A.A. Mukhin[3], and A.M. Balbashov[4]

[1] LURE, Centre Universitaire Paris-Sud, BP 34, 91898 Orsay Cedex, France
[2] Experimentalphysik V, Elektronische Korrelationen und Magnetismus, Institut für Physik, Universität Augsburg, 86135 Augsburg, Germany
[3] General Physics Institute, Russian Academy of Sciences, 105835 Moscow, Russia
[4] Moscow Power Engineering Institute, 105835 Moscow, Russia

Received 5 November 1999

Abstract. The optical conductivity of $La_{0.85}Sr_{0.15}MnO_3$ single crystals was studied by means of submillimeter and infrared spectroscopy for frequencies $4 < \nu < 15\,000\ \mathrm{cm}^{-1}$ and temperatures $10\ \mathrm{K} < T < 300\ \mathrm{K}$. The submillimeter conductivity follows the temperature dependence of the dc-data. The phonon spectrum of $La_{0.85}Sr_{0.15}MnO_3$ changes considerably below $T_C = 180$ K revealing a structural phase transition induced by charge or orbital order. At $T = 10$ K a number of phonon modes can be identified in addition to the room-temperature spectrum. The optical conductivity (σ_1) in the mid-infrared reveals the characteristics of small polaron absorption. Below the magnetic ordering temperature the polaron binding energy is highly reduced, but the onset of charge order interrupts the formation of free charge carriers with a Drude-like behavior. The frequency and temperature dependence of σ_1 in this regime qualitatively resembles the small polaron predictions by Millis *et al.* (Phys. Rev. B **54**, 5405 (1996)).

PACS. 63.20.-e Phonons in crystal lattices – 71.30.+h Metal-insulator transitions and other electronic transitions – 78.30.-j Infrared and Raman spectra

1 Introduction

Hole-doped manganese oxides with perovskite-type structure have long been known as prototypical metallic ferromagnets [1,2]. It is commonly believed that the ferromagnetic metallic state in these compounds is driven by Zener's double-exchange mechanism [3,4], originating from the strong Hund's-coupling between charge carriers and local spins. The physics of the manganese oxides has recently been revisited revealing new intriguing phenomena, such as colossal magnetoresistance effects (CMR) near the ferromagnetic transition temperature [5], charge and/or orbital ordered states [6–8], as well as field-induced structural transitions [9]. It has been shown theoretically that double-exchange alone cannot account for the sharp drop in resistivity just below the ferromagnetic transition and for the CMR effects [10,11]. Therefore, additional mechanisms have been suggested to be responsible for these observations, such as strong electron-phonon coupling [12], nonmagnetic randomness [13], phase separation effects [14] or strong hybridization between Mn $3d$ and O $2p$ orbitals [15].

Rather extensive literature on infrared properties of manganese oxides is available, reporting on the optical conductivity in systems with various dopant atoms and various doping concentrations. Examples of such studies are $La_{1-x}Sr_xMnO_3$ ($x = 0.1, 0.175$ and 0.30) [16,17], $La_{1-x}Ca_xMnO_3$ ($x = 0.3$ [18,19], $x = 0$ and 1 [20], $x = 0.33$ [21], $x = 0,\ 0.5$ and 0.67 [22]), $Nd_{0.7}Sr_{0.3}MnO_3$ [23], $Pr_{0.6}Ca_{0.4}MnO_3$ [24] and $La_{1.2}Sr_{1.8}Mn_2O_7$ [25]. Amongst the manganites, $La_{0.85}Sr_{0.15}MnO_3$ presents an extremely intriguing behavior. On the basis of recently published phase diagrams, the magnetic and structural properties close to the metal (M) to insulating (I) phase boundary ($x = 0.165$) of $La_{1-x}Sr_xMnO_3$ are by no means well established [8,26–28]. $La_{0.85}Sr_{0.15}MnO_3$ undergoes a rhombohedral to orthorhombic (O) phase transition close to 360 K and enters a magnetically ordered phase at 240 K. There is a controversy if this is a canted antiferromagnetic (CA) phase which is insulating [26] or a ferromagnetic (FM) and metallic phase (M) [8,27,28]. At approximately 200 K the compound undergoes a structural phase transition into an orthorhombic O″ structure which most probably is driven by charge or orbital order. In the recent literature this symmetry breaking phase transition is indexed as charge order (CO) transition. Concomitantly a FM and I ground state is established [8,26,27]. Between 240 K and 200 K the resistivity reveals a metallic like temperature dependence ($\mathrm{d}\rho/\mathrm{d}T > 0$). It is important to note that for

[a] *Present address*: Dipartimento di Fisica, Università di Roma "La Sapienza", P.le A. Moro 2, 00185 Roma, Italy
[b] also at CPMA, Université Paris-Sud, 91405 Orsay Cedex, France
[c] e-mail: andrei.pimenov@physik.uni-augsburg.de

the sample with a strontium concentration $x = 0.15$ no long-range Jahn-Teller (JT) distorted O′ phase appears which dominates the ground state properties at lower strontium concentrations ($0.1 < x < 0.15$).

In the present article we report on the optical properties of $La_{0.85}Sr_{0.15}MnO_3$ for temperatures 10 K $\leq T \leq$ 300 K. The energy range of measurements extends from the submillimeter frequencies, where the optical conductivity presents the same temperature dependence as the dc-conductivity, to the near infrared, where electronic transitions dominate the spectrum. In addition, we include the analysis of the far-infrared phonon modes.

2 Experimental details

The $La_{0.85}Sr_{0.15}MnO_3$ single crystals were grown by a floating zone method with radiation heating [29]. Raw La_2O_3, $SrCO_3$ and Mn_3O_4 chemicals of high purity (not less than 99.99%) were used for the preparation of ceramic rods. Some excess of Mn_3O_4 concentration (∼0.5 at.%) was used in order to compensate Mn losses due to the evaporation from the melt. The single crystals were grown in air atmosphere using a (110) growth direction. X-ray powder diffraction measurements showed that the crystals were single phase. Rocking curves from the (110) plane revealed half widths in the range from 30-80″. The misorientation of sub-blocks in the bulk of crystal did not exceed 1° with respect to the (110) direction. Two-dimensional X-ray topography of the samples indicated a twinned structure of the larger samples which were used in the optic investigations.

In the frequency range from 4 to 32 cm^{-1} transmission measurements were performed using a coherent source spectrometer [30] with a set of backward-wave oscillators (BWO) as monochromatic and continuously tunable sources. The measurements were performed in a Mach-Zehnder interferometer arrangement which allows measuring both the amplitude and the phase shift of the transmitted signal. Using Fresnel optical formulas, the conductivity and the dielectric constant were calculated directly from the observed spectra without any further approximations.

In the frequency range 23-15 000 cm^{-1} reflectance measurements were performed using a BOMEM DA 8 rapid scanning interferometer. Different sources, beamsplitters, detectors and optical windows allowed to cover the whole range. Synchrotron radiation was used in the far-infrared [31], while laboratory sources were used above 600 cm^{-1}. A gold-plated mirror served as a reference to evaluate the absolute reflectivity of the sample.

The samples were mounted on the cold finger of a liquid helium cryostat and the temperature was varied between 10 K and 300 K. Samples with thickness of ≈ 80 μ and ≈ 1 mm were used for transmission and reflectance measurements, respectively. Both samples were cut from the same single crystal.

The real part of the optical conductivity has been obtained from the reflectance measurements by means of Kramers-Kronig transformations. In the high frequency region between 16 000 cm^{-1} and 80 000 cm^{-1} the reflectivity as published by Okimoto *et al.* [16] was assumed. Above 80 000 cm^{-1}, a ω^{-4} extrapolation towards zero reflectivity was used. At frequencies between 4 and 25 cm^{-1}, the reflectance values were directly calculated from conductivity and the dielectric constant as measured in transmission geometry [32]. For frequencies below 4 cm^{-1} the reflectivity was evaluated from the data obtained by dielectric spectroscopy [33].

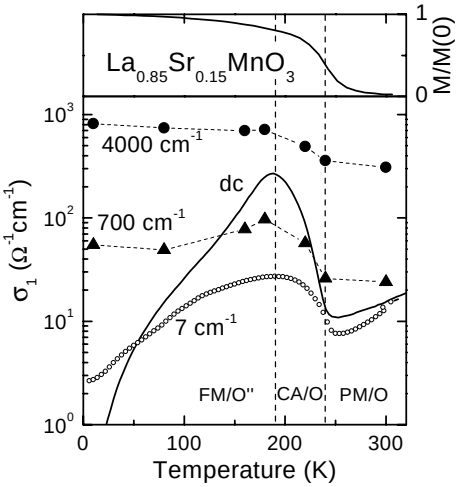

Fig. 1. Temperature dependence of the optical conductivity of $La_{0.85}Sr_{0.15}MnO_3$ at different frequencies (7 cm^{-1} (○)); 700 cm^{-1} (▲); 4000 cm^{-1} (●) as compared to the dc-conductivity (solid line). The normalized magnetization is indicated in the upper frame.

3 Results and discussion

Detailed studies of electrical resistivity $\rho(T)$ of $La_{1-x}Sr_xMnO_3$ have been published amongst others by Urushibara *et al.* [34], and Mukhin *et al.* [35]. With decreasing temperatures $\rho(T)$ in $La_{0.85}Sr_{0.15}MnO_3$ steadily increases for 1000 K $> T >$ 240 K and shows a small anomaly at 350 K which signals the structural phase transition from the high-temperature rhombohedral to the orthorhombic phase. A cusp like maximum close to 240 K indicates the onset of magnetic order and a minimum at 200 K the appearance of charge order. To characterize the sample under investigation we measured the dc conductivity ($\sigma_{dc} = 1/\rho_{dc}$) as a function of temperature. The result is shown as solid line in Figure 1. Below room temperature the dc-conductivity abruptly increases by more than one order of magnitude at the onset of magnetic order ($T_{CA} = 240$ K; here we use the nomenclature of Ref. [26]), but decreases again below $T_C = 190$ K which indicates the onset of the ferromagnetic and insulating ground state. Concomitantly, with the FM order the orthorhombic O″ phase is established, which probably reveals charge and orbital order. One possible realization of charge and orbital order is given by Paraskevopoulos *et al.* [26].

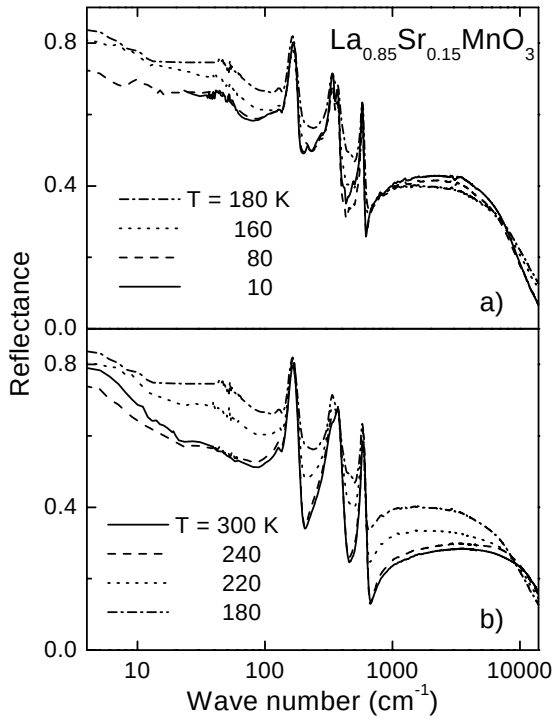

Fig. 2. Reflectivity spectra of $La_{0.85}Sr_{0.15}MnO_3$ at various temperatures. The spectra are shown separately for $T \leq 180$ K (a: upper frame) and for $T \geq 180$ K (b: lower frame).

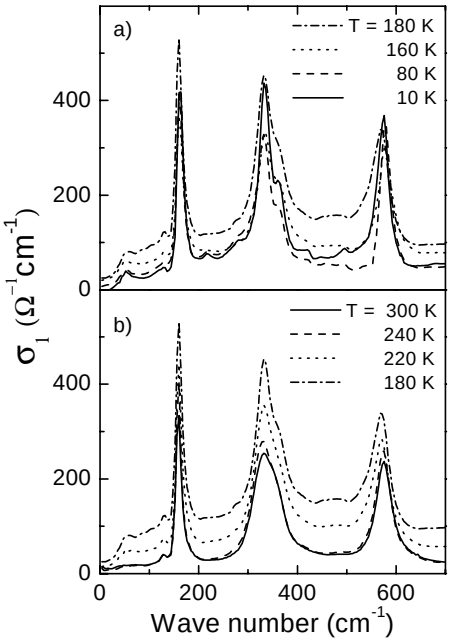

Fig. 3. Phonon part of the conductivity spectra of $La_{0.85}Sr_{0.15}MnO_3$ at various temperatures. The spectra are shown separately for $T \leq 180$ K (a: upper frame) and for $T \geq 180$ K (b: lower frame).

The reflectivity spectra of $La_{0.85}Sr_{0.15}MnO_3$ are reported in Figure 2 at various temperatures. For the reader's convenience the reflectivity spectra for $T \leq T_C$ (Fig. 2a) and for $T \geq T_C$ (Fig. 2b) are shown separately. Some general features are visible in the reflectance spectra. In the frequency region below 100 cm^{-1} the reflectivity slightly decreases as T decreases from 300 to 240 K, subsequently reaches a maximum at 180 K and decreases again at lower temperatures. In the far-infrared range, three main phonon features are present at all temperatures. In addition some weaker peaks evolve at low temperatures. In the following the optical conductivity in three frequency regions ($\nu < 50$ cm^{-1}, 100 $cm^{-1} < \nu < 600$ cm^{-1} and $\nu > 600$ cm^{-1}) will be presented in more details.

3.1 The spectral range $\nu < 50$ cm^{-1}

Qualitatively the submillimeter results follow the temperature behavior of the dc-conductivity. Figure 1 shows the optical conductivity obtained from the submillimeter measurements at 7 cm^{-1} as compared to the dc results. Again, on decreasing temperatures, the conductivity strongly increases below $T_{CA} = 240$ K, indicating the onset of magnetic order with a large ferromagnetic component (ferromagnetic or canted with a small canting angle). Below $T_C = 190$ K the ground state of $La_{0.85}Sr_{0.15}MnO_3$ becomes ferromagnetic and insulating [26] which results in temperature activated conductivity for frequencies below $\nu \sim 10$ cm^{-1} and at the lowest temperatures. For $T > T_{CA}$ the absolute value of dc conductivity approximately coincides with the submillimeter results, measured at a wave number of $\nu = 7$ cm^{-1}. This fact demonstrates that the resistivity is frequency independent in the paramagnetic phase. The strong decrease of σ_{dc} below 30 K indicates the dominance of hopping processes which are expected to reveal a power-law frequency dependence $\sigma \sim \nu^s$ with $s < 1$. The dc-conductivity is higher than $\sigma_1(7\ cm^{-1})$ around T_C. We believe that this is not indicative for the existence of a Drude-like behavior [32]. Possibly this observation reflects the large magnetic permeability around the magnetic phase transition temperature, which has been discussed in detail by Seeger *et al.* [33]. We also would like to point out that the frequency dependence for $x = 0.15$ is in marked contrast to the results obtained for $x = 0.125$ [26,32] where a strong hopping-like frequency dependence of the conductivity has been detected in the temperature range 10 K $< T <$ 300 K.

3.2 The spectral range 50 $cm^{-1} < \nu <$ 600 cm^{-1}

Figure 3 shows the optical conductivity of $La_{0.85}Sr_{0.15}MnO_3$ in the frequency range from 4 cm^{-1} to 700 cm^{-1}. At room temperature this spectral range is dominated by three main absorption bands centered at 160, 332 and 576 cm^{-1} (Fig. 3) which can be attributed to the extended phonons of the crystal [16,17]. Moreover, a small absorption line is visible at 124 cm^{-1} and the phonon line at 332 cm^{-1} is asymmetric. There is no major change in the far infrared conductivity above the magnetic transition, *i.e.* above $T_{CA} = 240$ K. As the temperature becomes lower, a wide electronic contribution superimposes onto the phonon absorption, reaching

its maximum close to T_C. Moreover, the phonon lineshape of the band at 350 cm^{-1} becomes more asymmetric and some weak absorption lines show up at 276 cm^{-1} and in the range 450-500 cm^{-1}. As the temperature decreases below $T_C = 190$ K, the electronic background decreases while the absorption line centered between 300 and 400 cm^{-1} splits at least into two components centered at 332 and 360 cm^{-1} and new but weaker lines appear in the far infrared region. At $T = 10$ K one can identify twelve contributions to the optical conductivity centered at 55, 128, 160, 216, 284, 332, 360, 420, 448, 496, 532 and 576 cm^{-1}.

Below room temperature $La_{0.85}Sr_{0.15}MnO_3$ transforms from the orthorhombic O phase to a new orthorhombic O$''$ phase [26]. Most probably the CA phase exists between $T_{CA} = 240$ K and $T_C = 190$ K, while the orbitally ordered phase O$''$ is stable in the ferromagnetic and insulating ground state. For a cubic crystal symmetry, three triply degenerated infrared active modes are expected, while a fourth triply degenerated mode is neither infrared nor Raman active [36]. The room temperature optical conductivity of the $La_{0.85}Sr_{0.15}MnO_3$ single crystal is in good agreement with this predictions as we observe three major phonon absorption bands. Weak orthorhombic distortions are likely causing the appearance of the weak line at 124 cm^{-1} as well as of the second component of the bending phonon causing the asymmetric lineshape.

As the crystal structure becomes distorted, the degeneracy of the phonon lines may be removed. Moreover, if the unit cell of the sample is not perfectly cubic, the fourth triply degenerated phonon may become infrared active, even if the intensity of this absorption line would remain weak. Such a behavior was observed in some rare earth perovskites which presents a slightly distorted structure compared to a cubic unit cell [36]. The orthorhombic distortions of manganites and their influence on the phonon spectrum were studied in the case of the O$'$ phase of $LaMnO_3$. For this compound Smirnova [37] calculated the Infrared and Raman active phonon modes. 25 IR active phonon were identified. In $La_{0.85}Sr_{0.15}MnO_3$, much more phonon modes can be identified at low temperatures compared to the room temperature spectrum. Two possible explanations can be given: One possibility is that the orthorhombic distortion increases at low temperatures in the O$''$ phase or that a superstructure evolves due to the evolution of charge and/or orbital order. The other one would be that the damping of the modes significantly decreases with decreasing temperature. However, before a detailed comparison with the phonon modes can be made a lattice dynamic calculations for the O$''$ structure are highly needed.

In a recent neutron scattering study, Yamada *et al.* [7] provided experimental evidence for a polaron ordered phase in a $La_{0.85}Sr_{0.15}MnO_3$. The onset temperature of the polaron order coincides with the point of resistivity upturn at T_C. The increasing appearance of the phonon modes below $T_C = 190$ K can probably be linked to the ordering of polarons on a periodic array which destroys the initial periodic crystal structure and lowers the crystal symmetry. Similar changes of crystal symmetries due to charge ordering below a transition temperature, T_{CO}, were observed by means of infrared spectroscopy measurements both in powders [38] and in single crystals [39] of $La_{1.67}Sr_{0.33}NiO_4$. Also in this compound the structural changes induced by the charge ordering transition split an intense phonon feature, which is centered around 350 cm^{-1} and is composed of degenerate modes, into its components. In the case of $La_{0.85}Sr_{0.15}MnO_3$, all the phonons of the crystal are affected by the charge ordering transition, indicating that the whole primitive cell is modified by the structural transition, as also observed in the case of $LiMn_2O_4$ [40].

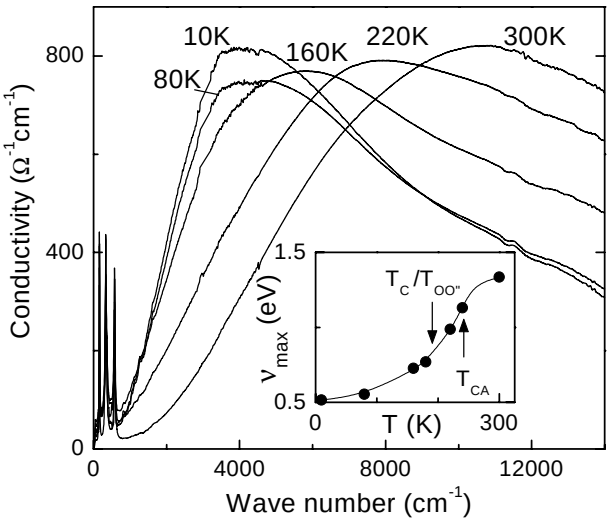

Fig. 4. Conductivity spectra of $La_{0.85}Sr_{0.15}MnO_3$ at various temperatures. The temperature dependence of the frequency of the conductivity maximum is given in the inset. The magnetic and structural phase transitions are indicated by arrows. The solid line in the inset is drawn to guide the eye.

Slight off-stoichiometry in our sample can be the origin of the small absorption band centered around 55 cm^{-1}, which is visible in Figure 3. This band is almost not discernible for $T \geq 240$ K, while it becomes visible at $T = 220$ K and its intensity increases as T is lowered to 10 K. At $T = 220$ K the real part of the dielectric function $\varepsilon_1(\nu = 7$ cm$^{-1})$ equals 40. Within a hydrogen atom impurity level frame [41] and taking into account this value of ε_1, we would expect an absorption band at about 65 cm^{-1}, a value which is in a reasonable agreement with the observed position. Another possible explanation for the structure at 55 cm^{-1} would be a phonon mode. However, the lowest IR active phonon mode in the O$'$ phase was calculated to appear at 76 cm^{-1} [37].

3.3 The spectral range $\nu > 600$ cm^{-1}

Figure 4 shows the optical conductivity of $La_{0.85}Sr_{0.15}MnO_3$ in the whole measured range. At room temperature the optical conductivity spectrum is dominated by a broad band centered at $\nu \sim 11\,000$ cm^{-1}. This band resembles relevant characteristics of a small

polaron. The small polarons are thought to be realized by electrons which are Jahn-Teller coupled to phonons. And indeed, $La_{0.85}Sr_{0.15}MnO_3$ is on the border line between the Jahn-Teller distorted O′-phase and the non-distorted O-phase, which probably reveals dynamic Jahn-Teller distortions. The peak maximum corresponds to a polaron binding energy of 1.4 eV. An electronic gap is visible which extends roughly to just above the phonon modes. As T decreases, the maximum of $\sigma(\nu)$ shifts to lower frequencies indicating a drastic reduction of the polaronic binding energy. This effect seems to be strongly enhanced in the canted phase. At $T \sim 80$ K the frequency position of the conductivity peak reaches its minimum value at about 4000 cm^{-1} and remains constant down to the lowest temperatures. The binding energy at the lowest temperatures approximately amounts 0.5 eV. The temperature dependence of the peak maximum which indicates the softening of the polaronic binding energies is shown in the inset of Figure 4. Clearly the polaronic states become increasingly weaker bound below the magnetic phase transition but the binding energies freeze in and become constant in the charge ordered phase. A strong transfer of spectral weight towards lower frequencies on decreasing temperatures has been observed for a variety of compounds: $La_{1-x}Sr_xMnO_3$ ($x = 0.1$, 0.2 and 0.3) [16,17], $La_{0.67}Ca_{0.33}MnO_3$ [21] and $La_{2-2x}Sr_{1+2x}Mn_2O_7$ [25]. However, the present conductivity results in $La_{0.85}Sr_{0.15}MnO_3$ provide clear experimental evidence for a considerable softening of the polaron binding energies.

The temperature evolution of the optical conductivity in $La_{0.85}Sr_{0.15}MnO_3$ qualitatively resembles the theoretical predictions of Millis *et al.* [12]. In these calculations the authors studied electrons which are coupled to phonons and, in addition, ferromagnetically to core spins. This model, which also contains the main essence of the colossal magnetoresistance, describes bound polarons in the case of strong electron-phonon coupling and a crossover to the Fermi-liquid like behavior for weaker coupling. $La_{0.85}Sr_{0.15}MnO_3$ is obviously on the border line between these two cases. In the CA phase (240 K $< T <$ 190 K) the polarons start to melt and the conductivity increases. Our experimental results clearly reveal this softening of the polaronic binding energy. The onset of charge order freezes in the polaron lattice and helps to establish a ferromagnetic and insulating ground state. However, some discrepancies with theoretical model calculations should be mentioned: In the work by Millis *et al.* [12], the small polaron absorption strongly increases at lower temperatures in the FM phase. This is not observed experimentally in Figure 4. In addition, when comparing our conductivity results to the small polaron calculations of Emin [42], we find an asymmetry in the polaronic absorption which is enhanced at higher frequencies, contrary to what is predicted theoretically. But we have to admit that a mid-infrared response may contribute to the conductivity in this range whose strength we can not estimate on the basis of the present results.

Finally, in Figure 1 we included the optical conductivity as observed at 4000 cm^{-1} and the magnetization data. On decreasing temperature, the infrared conductivity and the magnetization increase showing an abrupt change at the magnetic ordering temperature. This observation certainly documents the importance of the increased hopping probability of charge carriers in the ferromagnetically ordered phase and concomitantly a significant decrease of the polaron binding energies. Dynamical mean-field calculations within the double exchange model indicate that the spectral weight of intraband excitations within the lower exchange split-band is proportional to the second power of $M_{\rm norm}(T)$ [43].

3.4 The mid infrared energy gap and a possible Drude term

As mentioned in Section 3.3 and can be seen in Figure 4, at room temperature an energy gap is visible in the mid infrared conductivity spectrum around 700 cm^{-1}. This gap separates the phonon features in the far infrared range from the higher frequency electronic transitions and is due to the strong electronic correlations present in this material. The dc-conductivity of the presently studied $La_{0.85}Sr_{0.15}MnO_3$ sample (see Fig. 1) is much lower than the typical conductivity of a metal ($\sim 10^5$ Ω^{-1} cm^{-1}) so that no Drude term due to free charge-carriers is expected. And indeed the highest value of the DC conductivity is about 300 Ω^{-1} cm^{-1} for $T = 185$ K. Nevertheless, it is possible to identify a "metallic" state between $T_C = 190$ K and $T_{CA} = 240$ K, *i.e.* a temperature range in which ρ increases for increasing temperatures.

From Figures 2 and 3 it is evident that the optical conductivity at about 700 cm^{-1} increases by a factor of four as the temperature decreases from 240 K to 180 K and decreases monotonously on further cooling. Moreover the electronic contribution to the far infrared conductivity (in the phonon range) is much higher in the CA and "metallic" phase as compared to the conductivities at room temperature and below 180 K (see Fig. 3). With respect to this behavior, a partial delocalization of charge carriers, *i.e. via* an increase of the hopping probability, could be the reason for this so-called "metallic" state of $La_{0.85}Sr_{0.15}MnO_3$. However, certainly no Drude-like contribution can be identified in the submillimeter and far infrared spectra of the conductivity in this temperature range, and we believe that the softening of the binding energy of the small polarons is responsible for the increase of the dc conductivity in this "metallic" regime.

4 Conclusion

The present investigations of $La_{0.85}Sr_{0.15}MnO_3$ by means of submillimeter and infrared spectroscopies established links between various electronic, magnetic and structural properties observed in this compound. On the basis of the existing results we can exclude the existence of a Drude contribution. The charge ordering in the O″ phase causes a change of crystal symmetry as indicated by the splitting

of all the phonon lines visible in the far infrared. Concerning the electronic bands of $La_{0.85}Sr_{0.15}MnO_3$, a large transfer of spectral weight toward lower frequencies is evidenced as the temperature is decreased. We provide clear experimental evidence of a small polaron absorption at all temperatures investigated. The binding energy of the small polarons is strongly reduced at the onset of magnetic order, most probably due to the double-exchange mechanism. However, a structural phase transition into the O″ phase establishes charge order and interrupts the further melting of the polaronic conductivity into a Fermi-liquid behavior.

We wish to thank Christian Brouder, Ulrich Schneider and Emilio Orgaz for stimulating discussions, Joel Jaffré for technical support and Ross Gash for a critical reading of the manuscript. We are also grateful to CNRS and to the EEC for financial support for A. Paolone. This work was supported in part by BMBF *via* the contract EKM (13N6917/0) and by the European Community *via* INTAS (97-30850).

References

1. G.H. Jonker, J.H. van Santen, Physica **16**, 337 (1950); G.H. Jonker, J.H. van Santen, Physica **19**, 120 (1953).
2. E.O. Wollan, W.C. Koehler, Phys. Rev. **100**, 545 (1955).
3. C. Zener, Phys. Rev. **82**, 403 (1951); P.W. Anderson, H. Hasegawa, Phys. Rev. **100**, 675 (1955).
4. P.-G. de Gennes, Phys. Rev. **118**, 141 (1960).
5. M. Kusters, J. Singleton, D. A. Keen, R. McGreevy, W. Heyes, Physica B **155**, 362 (1989), R. von Helmolt, J. Wecker, B. Holzapfel, L. Schultz, K. Samwer, Phys. Rev. Lett. **71**, 2331 (1993); K. Chahara, T. Ohno, M. Kasai, Y. Kozono, Appl. Phys. Lett. **63**, 1999 (1993); S. Jin, T.H. Tiefel, M. McCormack, R. Fastnacht, R. Ramesh, L.H. Chen, Science **264**, 413 (1994),
6. Y. Tomioka, A. Asamitsu, Y. Moritomo, H. Kuwahara, Y. Tokura, Phys. Rev. Lett. **75**, 74, 5108 (1995).
7. Y. Yamada, O. Hino, S. Nohdo, R. Kanao, T. Inami, S. Katano, Phys. Rev. Lett **77**, 904 (1996).
8. J.-S. Zhou, J.B. Goodenough, A. Asamitsu, Y. Tokura, Phys. Rev. Lett. **79**, 3234 (1977)
9. A. Asamitsu, Y. Moritomo, Y. Tomioka, T. Arima, Y. Tokura, Nature **373**, 407 (1995).
10. A.J. Millis, P.B. Littlewood, B.I. Shraiman, Phys. Rev. Lett. **74**, 5144 (1995); Phys. Rev. B **54**, 5405 (1996).
11. H. Röder, J. Zang, A.R. Bishop, Phys. Rev. Lett. **76**, 1356 (1996).
12. A.J. Millis, Phys. Rev. B **53**, 8434 (1996); A.J. Millis, R. Mueller, B.I. Shraiman, Phys. Rev. B **54**, 5405 (1996).
13. L. Cheng, D.Y. Xing, D.N. Sheng, C.S. Ting, Phys. Rev. Lett. **79**, 1710 (1997).
14. S. Yunoki, J. Hu, A.L. Malvezzi, A. Moreo, N. Furukawa, E. Dagotto, Phys. Rev. Lett. **80**, 845 (1998).
15. D.I. Khomskii, G.A. Sawatzky, Solid State Commun. **102**, 99 (1997).
16. Y. Okimoto, T. Katsufuji, T. Ishikawa, T. Arima, Y. Tokura, Phys. Rev. B **55**, 4206 (1997).
17. Y. Okimoto, T. Katsufuji, T. Ishikawa, A. Urushibara, T. Arima, Y. Tokura, Phys. Rev. Lett. **75**, 109 (1995).
18. K.H. Kim, J.Y. Gu, H.S. Choi, G.W. Park, T.W. Noh, Phys. Rev. Lett. **77**, 1877 (1996).
19. K.H. Kim, J.H. Jung, T.W. Noh, Phys. Rev. Lett. **81**, 1517 (1998).
20. J.H. Jung, K.H. Kim, D.J. Eom, T.W. Noh, E.J. Choi, Jaejun Yu, Y.S. Kwon, Y. Chung, Phys. Rev. B **55**, 15489 (1997).
21. A.V. Boris, N.N. Kovaleva, A.V. Bazhenov, P.J.M. van Bentum, Th. Rasing, S.-W. Cheong, A.V. Samoilov, N.-C. Yeh, Phys. Rev. B **59**, R697 (1999).
22. P. Calvani, G. De Marzi, P. Dore, S. Lupi, P. Maselli, F. D'Amore, S. Gagliardi, S.-W. Cheong, Phys. Rev. Lett. **81**, 4504 (1998).
23. S.G. Kaplan, M. Quijada, H.D. Drew, D.B. Tanner, G.C. Xiong, R. Ramesh, C. Kwon, T. Venkatesan, Phys. Rev. Lett. **77**, 2081 (1996).
24. Y. Okimoto, Y. Tomioka, Y. Onose, Y. Otsuka, Y. Tokura, Phys. Rev. B **57**, R9377 (1998).
25. T. Ishikawa, T. Kimura, T. Katsufuji, Y. Tokura, Phys. Rev. B **57**, R8079 (1998).
26. M. Paraskevopoulos, F. Mayr, C. Hartinger, A. Pimenov, J. Hemberger, P. Lunkenheimer, A. Loidl, A.A. Mukhin, V.Yu Ivanov, A.M. Balbashov, J. Magn. Magn. Mater. **211**, 118 (2000); M. Paraskevopoulos, F. Mayr, J. Hemberger, P. Lunkenheimer, A. Loidl, A.A. Mukhin, V.Yu. Ivanov, A.M. Balbashov, J. Phys. Cond. Matter **12**, 1 (2000).
27. Y. Moritomo, A. Asamitsu, Y. Tokura, Phys. Rev. B **56**, 12190 (1997).
28. L. Vasiliu-Doloc, J.W. Lynn, A.H. Moudden, A.M. de Leon-Guevara, A. Revcolevschi, Phys. Rev. B **58**, 14913 (1998).
29. A.M. Balbashov, S.G. Karabashev, Ya.M. Mukovskii, S.A. Zverkov, J. Cryst. Growth **167**, 365 (1996).
30. A.A. Volkov, Yu.G. Goncharov, G.V. Kozlov, S.P. Lebedev, A.M. Prochorov, Infrared Phys. **25**, 369 (1985).
31. P. Roy, Y.-L. Mathis, A. Paolone, P. Giura, A. Nucara, S. Lupi, P. Calvani, A. Gerschel, Il Nuovo Cimento D **20**, 415 (1998); Y.-L. Mathis, P. Roy, B. Tremblay, A. Nucara, S. Lupi, P. Calvani, A. Gerschel, Phys. Rev. Lett. **80**, 1220 (1998).
32. A. Pimenov, Ch. Hartinger, A. Loidl, A.A. Mukhin, V.Yu. Ivanov, A.M. Balbashov, Phys. Rev. B **59**, 12419 (1999).
33. A. Seeger, P. Lunkenheimer, J. Hemberger, A.A. Mukhin, V.Yu. Ivanov, A.M. Balbashov, A. Loidl, J. Phys. Cond. Matter **11**, 3273 (1999).
34. A. Urushibara, Y. Moritomo, T. Arima, A. Asamitsu, G. Kido, Y. Tokura, Phys. Rev. B **51**, 14103 (1995).
35. A.A. Mukhin, V.Yu. Ivanov, V.D. Travkin, S.P. Lebedev, A. Pimenov, A. Loidl, A.M. Balbashov, JETP Lett. **68**, 356 (1998).
36. M. Couzi, P. Van Huong, J. Chim. Phys. (France) **69**, 1339 (1972).
37. I.S. Smirnova, Physica B **262**, 247 (1999).
38. P. Calvani, A. Paolone, P. Dore, S. Lupi, P. Maselli, P.G. Medaglia, S.-W. Cheong, Phys. Rev. B **54**, R9592 (1996).
39. T. Katsufuji, T. Tanabe, T. Ishikawa, Y. Fukuda, T. Arima, Y. Tokura, Phys. Rev. B **54**, R14230 (1996).
40. A. Paolone, P. Roy, G. Rousse, C. Masquelier, J. Rodriguez-Carvajal, Solid State Commun. **111**, 453 (1999).
41. N.W. Ashcroft, N.D. Mermin, in *Solid State Physics* (Ed. Saunders College, Philadelphia, 1976).
42. D. Emin, Phys. Rev. B **48**, 13691 (1993).
43. N. Furukawa, J. Phys. Soc. Jpn **64**, 3164 (1995).